Theoretical analysis and numerical computation of dilute solid/liquid two-phase pipe flow

FU Xudong (傅旭东), WANG Guangqian (王光谦)
& DONG Zengnan (董曾南)

Department of Hydraulic Engineering, Tsinghua University, Beijing 100084, China

Received September 20, 2000

Abstract Starting with the kinetic theory for dilute solid/liquid two-phase flow, a mathematical model is established to predict the flow in a horizontal square pipe and the predictions are compared with LDV measurements. The present model predicts correctly two types of patterns of the vertical distribution of particle concentration observed in experiments, and also gives different patterns of the distribution of particle fluctuating energy. In the core region of the pipe, the predicted mean velocity of particles is smaller than that of liquid, but near the pipe bottom the reverse case occurs. In addition, full attention is paid to the mechanism for the vertical distribution of the average properties of particles such as concentration and mean velocity. From the kinetic-theory point of view, the cause of formation for different patterns of the vertical concentration distribution is not only related to the lift force exerted on a particle, but also related to the distribution of particle fluctuating energy.

Keywords: **solid/liquid two-phase flow, kinetic theory, mathematical model.**

A solid/liquid two-phase flow system can be described either in terms of a microscopic method (kinetic theory) or macroscopic method (continuum theory)[1,2]. In the past two or three decades, the kinetic theory has been rapidly developed for gas/solid and granular flows, and also introduced into some solid/liquid flow systems. Wang and Ni[3,4] adopted the kinetic theory in their studies. They regarded the solid particles as analogous to molecular of gas in gas kinetic theory and described them by the Boltzmann equation. Taking a variation method to solve the equation, the authors obtained an explicit particle velocity distribution function and a theoretical formula for the vertical distribution of particle concentration. The formula agreed with the experiment data in square pipe flow very well. However, so many assumptions were taken in their analysis, and the results left much to be improved. Based on the kinetic theory for granular flows, Ding and Gidaspow[5] considered the forces on a particle including the drag force, gravitational force and buoyancy force, and deduced the balance equations for particle phase, and successfully predicted the bubble motion in rapid fluidization bed. In their investigation, both the lift force on a particle and the fluctuating velocity correlation of two phases are ignored. Louge et al.[6] and Cao and Ahmadi[7] introduced the kinetic theory for granular flows into the turbulent gas-solid two-phase flows in a vertical pipe. Both of them used similar boundary conditions and only considered the interphase drag force and the gravitational force. In solid/liquid two-phase flows, however, the forces on a particle are very complex, and the lift force, the interphase drag force and the gravity are all very important. In the present study, we try to employ the kinetic theory to investigate the properties of particle phase, with the forces on particles thoroughly considered in dilute

solid/liquid two-phase square pipe flow, and compare the predictions with LDV measurements.

1 Basic theory

1.1 General equations

For uniform, spherical, coarse particles in dilute solid/liquid flows, assuming nearly elastic and frictionless interparticle collisions and considering the influence of the interphase forces on particle motion, the particle phase can be described using the modified granular equations given by Jenkins and Savage[8] as follows[6]:

continuum equation

$$\frac{\mathrm{d}\rho}{\mathrm{d}t} + \rho \frac{\partial \nu}{\partial x_i} = 0, \tag{1}$$

momentum equation

$$\rho \frac{\mathrm{d}\nu_i}{\mathrm{d}t} = \rho \langle F_i \rangle - \frac{\partial P_{ji}}{\partial x_j}, \tag{2}$$

fluctuating energy equation

$$\frac{3}{2}\rho \frac{\mathrm{d}T}{\mathrm{d}t} = \rho \langle F_i C_i \rangle - P_{ij} \frac{\partial \nu}{\partial x_i} - \frac{\partial q_i}{\partial x_i}, \tag{3}$$

where $\rho = nm$ represents the bulk density of particle phase, m the mass of a particle, n the number of particles per unit volume; $\langle \cdot \rangle$ denotes an ensemble average, $P_{ij} = \rho \langle C_i C_j \rangle$ the fluctuating stress in particle phase, $C_i = c_i - \nu_i$ the particle fluctuating velocity, c_i the stochastic velocity, ν_i the average velocity, $q_i = \frac{1}{2}\rho \langle C^2 C_i \rangle$ the particle fluctuating energy flux, $T = \frac{1}{3}\langle C_i C_i \rangle$ the "granular temperature", $\langle F_i \rangle$ are the external forces per unit mass on a particle, including both the body force and the action forces on a particle by the liquid, and $\langle F_i C_i \rangle$ is the correlation between the forces on unit mass particle and the particle fluctuating velocity.

Let the volume concentration of particles be ε, the material density of particles be ρ_s and the particle fluctuating energy be k. Then ρ and T also can be expressed as

$$\rho = \varepsilon \rho_s, \quad T = \frac{2}{3}k. \tag{4}$$

And the corresponding constitutive relations to the balance equations above are[6,8]

$$P_{ij} = \left(\rho T + \frac{2\mu}{3}\frac{\partial \nu}{\partial x_k}\right)\delta_{ij} - \mu\left(\frac{\partial \nu_i}{\partial x_j} + \frac{\partial \nu_j}{\partial x_i}\right), \tag{5}$$

$$q_i = -\lambda \frac{\partial T}{\partial x_i}, \tag{6}$$

where δ_{ij} is the second order unit tensor, and μ and λ are the coefficients of viscosity and fluctuating energy flux, respectively.

1.2 Governing equations for 2D flows

For dilute, fully developed, steady solid/liquid two-phase flows in a horizontal square pipe, the flow along the perpendicular bisector of the pipe is considered as two-dimensional (fig. 1). Hence, both the time and spatial derivatives of flow properties in the flowing direction are zero, and only the streamwise particle velocity remains:

$$\frac{\partial}{\partial t} = 0, \quad \frac{\partial}{\partial x} = 0, \quad \nu_y = 0, \quad \nu_x = \nu(y).$$

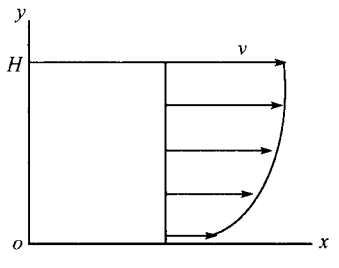

Fig. 1. The sketch of 2D steady, uniform solid/liquid two-phase flow.

Under the above simple flow conditions, the set of governing equations (1)—(3) are simplified into

x-momentum equation:

$$\rho \frac{F_{0x}}{m} + \frac{\partial}{\partial y}\left(\mu \frac{\partial \nu}{\partial y}\right) = 0, \tag{7}$$

y-momentum equation:

$$\rho \frac{F_{0y}}{m} - \frac{\partial(\rho T)}{\partial y} = 0, \tag{8}$$

fluctuating energy equation:

$$\rho\langle F_i C_i\rangle + \mu \frac{\partial \nu}{\partial y}\frac{\partial \nu}{\partial y} + \frac{\partial}{\partial y}\left(\lambda \frac{\partial T}{\partial y}\right) = 0, \tag{9}$$

where $F_{0x} = m\langle F_x\rangle$ and $F_{0y} = m\langle F_y\rangle$) are the mean external forces on a particle in the x and y directions, respectively, including the gravitational force and interphase forces. Considering the dilute flow of relatively massive particles, the corrected expressions for μ and λ proposed by Louge et al.[6] for such a simple flow are

$$\mu = \frac{5\sqrt{\pi}}{96}\rho_s d_p T^{1/2}\frac{1}{1 + \lambda/H}, \tag{10}$$

$$\lambda = \frac{25\sqrt{\pi}}{128}\rho_s d_p T^{1/2}\frac{1}{1 + \lambda/H}, \tag{11}$$

where $\lambda = d_p/6\sqrt{2\varepsilon}$ is the characteristic length of particles between two successive collisions, d_p is particle diameter, and H is the half depth of the square pipe.

In the flowing direction, assuming that the streamwise pressure gradient in the flow field is so small that it can be ignored, the mean external force F_{0x} is mainly from the drag of liquid phase. Taking into account the wall effects, the Faxen's correction is used and F_{0x} can be approximated by the drag formula for steady flows:

$$F_{0x} = \frac{1}{8}\pi C_1 C_D d_p^2 \rho_f \mid u - \nu \mid (u - \nu), \tag{12}$$

where ρ_f is the liquid density, μ is the mean velocity of liquid; C_D is the drag coefficient, related to the particle Reynolds number Re_p; C_1 is the correction factor of Faxen[9]:

$$C_1 = \left[1 - \frac{9}{16}\left(\frac{d_p}{2y}\right) + \frac{1}{8}\left(\frac{d_p}{2y}\right)^3 - \frac{45}{256}\left(\frac{d_p}{2y}\right)^4 - \frac{1}{16}\left(\frac{d_p}{2y}\right)^5\right]^{-1}, \tag{13}$$

$$C_D = \frac{24}{Re_p} f(Re_p), \tag{14}$$

$$Re_f = \frac{\rho_f d_p \mid u - \nu \mid}{\mu_f}, \tag{15}$$

$$f(Re_p) = 1 + 0.15 Re_p^{0.687} + 0.0175(1 + 4.25 \times 10^4 Re_p^{-1.16})^{-1}. \tag{16}$$

Formula (16) is the drag factor or the ratio of the drag coefficient to Stokes drag, which is proposed by Clift and Gauvin and is accurate over the entire subcritical Reynolds number range[10]. Define the hydrodynamic relaxation time, τ_ν, for a particle as follows:

$$\frac{1}{\tau_\nu} = \frac{3}{4}\frac{\rho_f}{\rho_s}\frac{C_D}{d_p} \mid u - \nu \mid. \tag{17}$$

Then the average external force in the x direction in eq. (7) can be expressed simply as

$$\frac{F_{0x}}{m} = \frac{u - \nu}{\tau_\nu}. \tag{18}$$

In the vertical direction, the external force on a particle consists of many forces, such as the gravitational force, drag force, pressure gradient force, virtual mass effect, and the lift forces due to the velocity gradient and particle rotation, etc. Owing to the lack of successful treatment to determine any of them in particle-liquid system, all the vertical forces acting on a particle by the liquid are taken as a comprehensive lift force, just as done by Wang and Ni[4]. According to Owen[11], the comprehensive lift force by the liquid on a coarse particle can be expressed as

$$L_f - \rho_f(u -) d_p^3 \frac{du}{dy} \sim \frac{\rho_f}{\rho_s} m \frac{du}{dy}(u - \nu) = \alpha' \frac{\rho_f}{\rho_s} m \frac{u_*^2}{y}, \tag{19}$$

where u_* is the shear velocity of two phase flow, $\alpha' = 1.2(gd_p/\omega u_*)(1 - \rho_f/\rho_s)(\rho_s/\rho_f)^{1/2}$ a coefficient of the lift force[12], ω the particle settling velocity in quiescent water, and y the distance from pipe bed. Including the effective gravitational force, the total vertical external force per unit mass on a particle is

$$\frac{F_{0y}}{m} = \alpha' = \frac{\rho_f}{\rho_s} \frac{u_*^2}{y} - \left(1 - \frac{\rho_f}{\rho_s}\right) g, \tag{20}$$

where the second term on the right-hand side is the effective gravitational force, and g is the acceleration of gravity.

In the fluctuating energy equation of (9), $\rho\langle F_i C_i\rangle$ is the average power of the external force on the fluctuating motion of particles. According to the analysis of Liu[1], the forces related to the particle velocity by the liquid can be divided into two parts. One part is in the direction of the particle velocity, and the other is in the perpendicular direction and does not contribute to $\rho\langle F_i C_i\rangle$ (the dot product is zero). Hence the average power, $\rho\langle F_i C_i\rangle$, is approximately[13]:

$$\rho\langle F_i C_i\rangle = \frac{\rho}{\tau_\nu}\langle u_i' C_i\rangle - 3\frac{\rho}{\tau_\nu} T, \tag{21}$$

where u_i' is the liquid fluctuating velocity, and the first term on the right-hand side is the coupling of two-phase fluctuating velocities. Koch[14] has proposed a theoretical formula for very dilute gas/solid flow with little Reynolds number, $Re_p < 1$, and large Stokes number, St, with the the hydrodynamics effect considered

$$\langle u_i' C_i\rangle = \frac{d_p \mid u_i - \nu_i \mid \mid u_i - \nu_i \mid}{4\sqrt{\pi}\tau_S \sqrt{T}}, \tag{22}$$

where τ_S is particle Stokes relaxation time. In the square pipe flow we investigated, Re_p is much greater than 1, and no theoretical formula is available for such a case[15]. As the preliminary treatment, following Louge et al.[6], we take the form of formula (22), but change τ_S into the particle hydrodynamic relaxation time τ_ν.

1.3 Boundary conditions

In two-phase pipe flow, collisions between particles and the wall often take place, making the momentum and energy exchange between them. By considering the momentum and energy balance of an infinitesimal volume on the wall, Jenkins[16] calculated the boudary conditions for the particle phase, and the result has been used successfully by Louge et al.[6] and Cao and Ahmadi[7] in gas/solid two-phase flows. In solid/liquid two-phase flow in a smooth square

pipe[3,4], it can be assumed that the collisions are always sliding and slightly frictional. And the tangential stress, S_b, and the normal stress, N_b, are given as[6,7,16]:

$$S_b = -\mu_w N_b. \tag{23}$$

And the particle fluctuating energy flux on the boundary, q_b, takes the form

$$q_b = -\frac{3}{8} N_b \sqrt{3T_b}\left[\frac{7}{2}(1+e_w)\mu_w^2 - (1-e_w)\right] \tag{24}$$

where the subscript b denotes the value on the boundary, μ_w and e_w are the sliding coefficient and the coefficient of restitution for a particle colliding with the wall, respectively. In the present model, the two coefficients take the values of 0.2 and 0.7, respectively, as done by the previous investigators[6,7]. The tangential stress, S, and the normal stress, N, are as follows:

$$S = \mu \frac{\partial v}{\partial y}, N = \rho T. \tag{25}$$

In order to compare the model predictions with the experiments, the measured data of particle concentration is employed as the known boundary value at the bottom of the square pipe.

2 Equation discretization

A computational 2D (two-dimensional) grid system should be set up longitudinally along the perpendicular bisector of the pipe. Due to the uniformity of the flow in the flowing direction, the 2D grid system reduces to the 1D one, as shown in fig. 2(a). A staggered grid system is used. The variables of two-phase velocities, $\boldsymbol{u}$ and $\boldsymbol{v}$, are stored at velocity nodes and the particle bulk density, ρ, and granular temperature, T, are stored at density grid points.

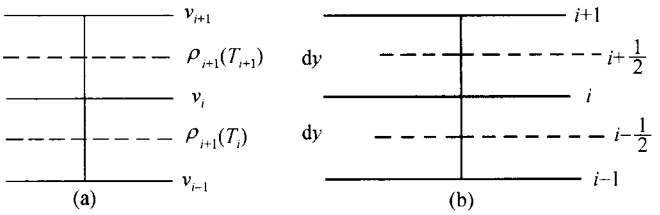

Fig. 2. The sketch of the grid system and equation discretization. (a) A staggered grid system; (b) equation discretization.

Both eqs. (7) and (9) are discretized after integrating in computational domain first. For the sake of brevity, we only discretize eq. (7) in detail. At the node i in the v-grid system, as shown in fig. 2(b), integrating by eq. (7) over the interval of $\left[i-\frac{1}{2}, i+\frac{1}{2}\right]$, we obtain

$$\int_{i-\frac{1}{2}}^{i+\frac{1}{2}} \rho \frac{F_{0x}}{m} dy + \left(\mu \frac{\partial v}{\partial y}\right)\Big|_{i-\frac{1}{2}}^{i+\frac{1}{2}} = 0. \tag{26}$$

Taking the value of function $\rho(F_{0x}/m)$ at grid i to approximate its average value in the interval, the above equation takes the form

$$\left(\rho \frac{F_{0x}}{m}\right)_i dy + \left(\mu \frac{\partial v}{\partial y}\right)_{i+\frac{1}{2}} - \left(\mu \frac{\partial v}{\partial y}\right)_{i-\frac{1}{2}} = 0. \tag{27}$$

Utilizing a central difference to approximate the velocity gradient in eq. (27), and substituting eq. (18) into eq. (27), the discretized equation of eq. (7) is obtained:

$$a_i v_i + b_i v_{i+1} + c_i v_{i-1} = d_i, \tag{28}$$

where

$$a_i = \frac{\rho_i}{\tau_{vi}}\mathrm{d}y\mathrm{d}y + \mu_{i+\frac{1}{2}}\mu_{i-\frac{1}{2}}, \quad b_i = -\mu_{i+\frac{1}{2}}, \quad c_i = -\mu_{i-\frac{1}{2}}, \quad d_i = \frac{\rho_i}{\tau_{vi}}u_i\mathrm{d}y\mathrm{d}y.$$

The bulk density ρ_i at node i in the v-grid system should be evaluated through interpolation with the known values in the density grids. According to fig. 2(a), the particle bulk density, $\rho_i|_v$, in v-grid system is

$$\rho_i|_v = 2\frac{\rho_i\rho_{i+1}}{\rho_i + \rho_{i+1}}\bigg|_\rho. \tag{29}$$

In a similar way, eq.(9) is discretized in the density grid system as follows:

$$\left(\lambda_{i+\frac{1}{2}} + \lambda_{i-\frac{1}{2}} + 3\frac{\rho_I}{\tau_{vi}}\right)T_i - \lambda_{i+\frac{1}{2}}T_{i+1} - \lambda_{i-\frac{1}{2}}T_{i-1}$$
$$= \left(\frac{\rho}{\tau_v}\langle u_k'C_k\rangle\right)_i \mathrm{d}y\mathrm{d}y + \mu_i\left(\nu_{i+\frac{1}{2}} - \nu_{i-\frac{1}{2}}\right)^2. \tag{30}$$

Eq.(8), the momentum equation in the y direction, includes two variables of ρ and T. It can be discretized in the density grid system. And as only the first order derivative terms exist, this equation can be rewritten as

$$\frac{\partial\rho}{\partial y} = \frac{\rho}{T}\left(\frac{F_{0y}}{m} - \frac{\partial T}{\partial y}\right). \tag{31}$$

It can be solved by the classic four-order Rouge-Kutta method.

3 Results and discussions

Wang[12] has investigated the solid/liquid two-phase flow in a smooth square pipe by means of laser doppler anemometer (LAD). The pipe size is 4×6 cm^2, and nearly neutral polystyrene particle ($\rho_s = 1050$ kg/m^3) and heavy cation resin particle ($\rho_s = 1600$ kg/m^3) were used, with diameter d_p ranging from 0.6 to 2.29 mm. The shear velocity u_* varies from 3.21 to 7.43 cm/s, the average volume ratio $\bar{\epsilon}$ is 0.01—1.34% and the maximum local concentration is 5%.

3.1 Liquid velocity

The experiment shows that the clear water does not exactly exhibit a vertical velocity profile of logarithmic distribution in the square pipe flow, and a wake term should be added with the intensity $\Pi = 0.2$. The modified Dou's formula[17] for clear water is

$$\frac{u}{u_*} = 2.5\ln\left(1 + \frac{u_* y}{5\nu}\right) + 7.05\left[\frac{u_* y}{5\nu}\Big/\left(1 + \frac{u_* y}{5\nu}\right)\right]^2 + 2.5\left[\frac{u_* y}{5\nu}\Big/\left(1 + \frac{u_* y}{5\nu}\right)\right]$$
$$+ 25\Pi\left[1 - \cos\left(\pi\frac{y}{H}\right)\right], \tag{32}$$

where $H = 2$ cm is the half depth of square pipe. In this experiment, the flow is dilute and the maximum local volume ratio is not more than 5%. Therefore, it could be assumed that particles have only little influence on the mean flow properties of liquid, and the velocity profile of liquid can still be described by formula (32). This assumption proves to be reasonable by the experimental results. Fig. 3(a) is a comparison between the predicted and the measured data for clear water; fig. 3(b) is a comparison for two-phase flows under different situations. In the present model, the above formula is employed to calculate the liquid velocity profile directly.

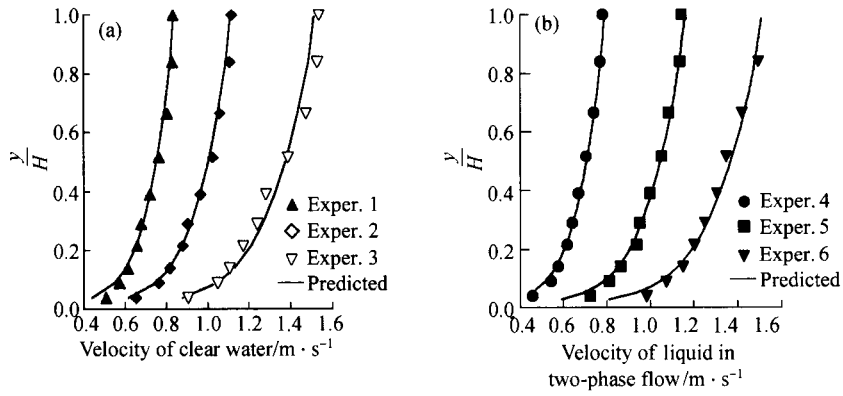

Fig. 3. Velocity profiles of liquid in solid/liquid two-phase pipe flow. 1, $u_* = 3.66$ cm/s, $\bar{\varepsilon} = 0$; 2, $u_* = 4.72$ cm/s; 3, $u_* = 6.25$ cm/s, $\bar{\varepsilon} = 0$; 4, $u_* = 3.47$ cm/s, $\bar{\varepsilon} = 0.77\%$; 5, $u_* = 4.90$ cm/s, $\bar{\varepsilon} = 0.06\%$; 6, $u_* = 6.23$ cm/s, $\bar{\varepsilon} = 0.04\%$.

3.2 Particle concentration distribution

The vertical distribution of particle concentration exhibits two types of patterns, called pattern I and pattern II. The former shows a pattern that there is the maximum concentration at some location above the bottom and the concentration below this location decreased. The latter always shows an increase in the particle concentration downward over the whole vertical, with the maximum value at the bottom. Both of these two patterns were observed in Wang's experiment. Fig. 4 compares the predicted and measured profiles of particle concentration. As shown in this figure, the present model predicts correctly the profiles of particle concentration in different situations. Under the assumption of uniform distribution of particle fluctuating energy, Wang and Ni[4] attributed the formation of two patterns to the lift force exerted on a particle. According to eq. (31), when T is of uniform distribution in the vertical direction, that is, $\partial T/\partial y$, the derivative $\partial \rho/\partial y$ is zero if $F_{0y}/m = 0$ is satisfied at some location of y above the bottom. In such a way,

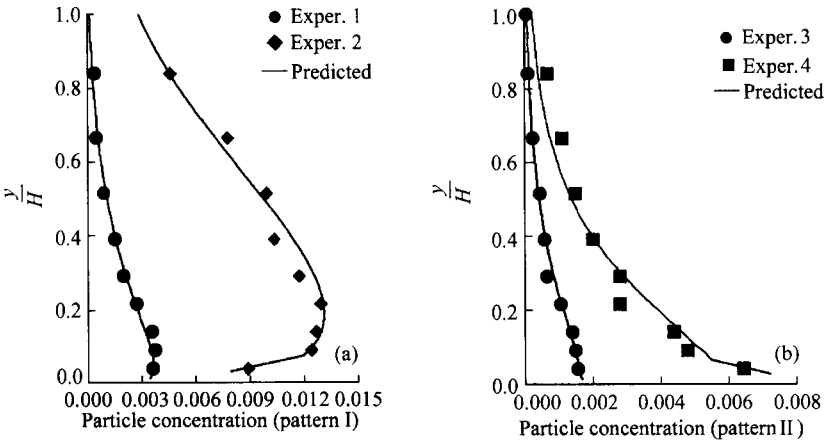

Fig. 4. Profiles of particle concentration in solid/liquid two-phase pipe flow. 1, Cation resin $u_* = 4.95$ cm/s, $\bar{\varepsilon} = 0.14\%$, $d_p = 0.6$ mm; 2, polystyrene $u_* = 3.43$ cm/s, $\bar{\varepsilon} = 0.88\%$, $d_{p*} = 1.3$ mm; 3, cation resin $u_* = 4.90$ cm/s, $\bar{\varepsilon} = 0.06\%$, $d_p = 0.6$ mm; 4, cation resin $u_* = 6.15$ cm/s, $\bar{\varepsilon} = 0.20\%$, $d_p = 1.1$ mm.

the concentration profile has an extremum at y and pattern I appears. In addition, we rewrite eq. (20) into the following form:

$$F_{0y}/m(\rho_f/\rho_s)(\alpha' u_*^2/y + g) - g. \tag{33}$$

By eq. (33), if the material density of particles, ρ_s, is relatively small, the ratio ρ_f/ρ_s will be large. Keep other parameters unchanged. Then the function F_{0y}/m will get a large value correspondingly, thus making $\partial\rho/\partial y$ have a trend towards a positive value. If $F_{0y}/m \geqslant 0$ is reached, $\partial\rho/\partial y \geqslant 0$ and pattern I appears. From this point of view, particles with smaller density are more likely to form the concentration distribution of pattern I. This is consistent with Wang and Ni[4]'s result and agrees with the experiments. However, under general flow conditions the derivative $\partial T/\partial y$ does not take the value of zero. According to eq. (31), $\partial T/\partial y < 0$ will make $\partial\rho/\partial y$ nonnegative, and therefore increase the possibility of the occurrence of pattern I. In contrast, $\partial T/\partial y > 0$ will contribute to a negative value of $\partial\rho/\partial y$ and consequently to the occurrence of pattern II. Therefore, it can be seen that the detailed profiles of particle concentration are not only determined by the lift force, but also by the distribution of granular temperature T.

3.3 Particle velocity distribution

Fig. 5 shows the average measured and predicted particle velocities. The predicted value is close to that of the measured in the core region and the mean particle velocity is less than that of liquid. But near the bed, there are some discrepancies between the predictions and the experiments, and the predicted value may be larger than that of liquid. As far as the drag force related to the relative velocity between the two phases is concerned, the smaller relative velocity indicates a smaller value of drag force on a particle in the present model. It may relate to two factors. The first is the average velocities used in formula (12) to approximate the instantaneous values to get the ensemble average drag force on a particle. The second is that only the drag force was considered and both the Basset force and virtual mass effect were ignored. With respect to the discrepancies near the bed, boundary conditions used here may have some influences on them besides the two reasons just mentioned above. In terms of physical mechanism, the liquid velocity meets the no-slip condition at the wall, but slip velocity exists for particle phase because the streamwise particle velocity partly remains after the collisions. As a result, a region may appear near the wall where the mean velocity of particles is greater than that of liquid. For solid/liquid two-phase flows, this region may be small due to the slight difference between the densities of two phases. And this region was found by many investigators in their experiments[18—20]. In Wang's experiment, as the lowest measuring point is 0.8mm above the bed, such a region may not be observed. In the present study, boundary treatment only reflects the effect of collisions between the wall and particles, but does not take into account the effect of interphase forces on the whole process of collisions. This may make the region larger.

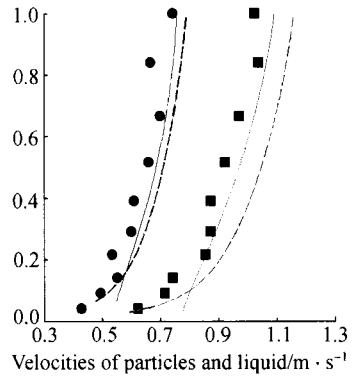

Fig. 5. Profiles of the mean velocities in solid/liquid two-phase pipe flow. ●, Experiment for partcles 1; ■, expeiment for particles 2; ——, predicted for particles; ·····, predicted for liquid. Particles 1, polystyrene $u_* = 3.47$ cm/s, $\bar{\varepsilon} = 0.77\%$, $d_p = 1.3$ mm; particles 2, cation resin $u_* = 4.90$ cm/s, $\bar{\varepsilon} = 0.06\%$, $d_p = 0.6$ mm.

3.4 Particle fluctuating energy distribution

The predicted particle fluctuating energy is displayed in fig. 6, where the dimensionless coordinate of fluctuating energy is expressed as $(\langle C_iC_i \rangle)^{1/2}/u_*$. The prediction shows several kinds of distribution patterns in the mainstream. Fig. 6(a) displays the pattern of nearly linear distribution, and fig. 6(b) gives some distributions in a reverse "C" type. The two types of patterns are similar to those of particle concentration. According to eqs.(9) and (21), the particle fluctuating energy consists of the shearing energy from the mean velocity field, the diffusion of the fluctuating energy, the correlation of two-phase fluctuating velocities and the work done by drag force. These factors determine the patterns of fluctuating energy distribution. And in the same figure, the predicted energy is larger near the bottom but smaller in the core region. This can be explained by the fact that interparticle collisions and collisions between particles and the wall often take place near the bed. In addition, the turbulent bursting also has serious influence on particle motion in this region. As a result, the particle fluctuating energy becomes larger. Unfortunately, we cannot compare our predictions of the profiles of particle fluctuating energy with the experiments of Wang, who did not measure the velocity fluctuations of particles. But the predicted results agree with the experiments of Van de Wall and Soo[21] qualitatively.

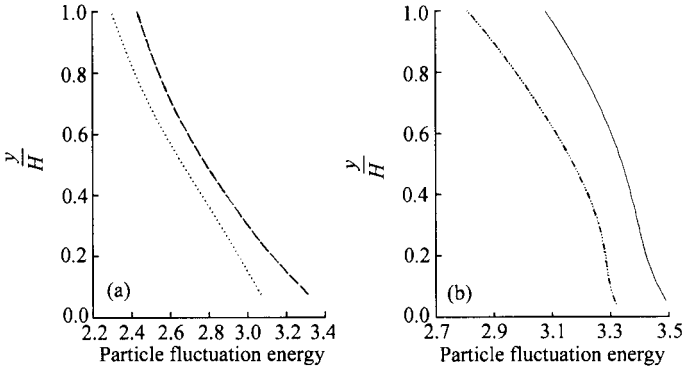

Fig. 6. Profiles of particle fluctuation energy in solid/liquid two-phase pipe flow. ·····, polystyrene $u_* = 3.47$ cm/s, $\bar{\varepsilon} = 0.77\%$, $d_p = 1.3$ mm; - . - ., polystyrene $u_* = 3.43$ cm/s, $\bar{\varepsilon} = 0.88\%$, $d_p = 1.3$ mm; - .. - .. -, cation resin $u_* = 6.21$ cm/s, $\bar{\varepsilon} = 0.05\%$, $d_p = 0.6$ mm; ——, cation resin $u_* = 7.34$ cm/s, $\bar{\varepsilon} = 0.14\%$, $d_p = 0.85$ mm.

3.5 Discussions

In the present study, the set of simplified equations (7)—(25) are obtained with the original general equations for dilute, fully developed, steady solid/liquid two-phase flow in a square pipe. And the reduction in the coupling of bulk density (or particle concentration), mean velocity and granular temperature (or particle fluctuating energy) benefits our numerical computation. But it should be stated that there is no theoretical formula for the coupling term of the fluctuating velocities, $\langle u'_iC_i \rangle$, in solid/liquid two-phase flows until now. And the lack of corresponding experiment data makes the selection of the formula for this coupling more experiential. Though the theoretical formula proposed by Koch[14] is modified and used by Louge et al.[6] in turbulent gas/solid two-phase flow, it is still of serious deficiency. For example, when the relative velocity between the two phases is zero; that is, the particle follows the liquid motion closely, this formula predicts zero value, and it is obviously unreasonable. Giving up the modification by Louge et al.[6] and replacing the term of $(u_i - v_i)(u_i - v_i)$ in eq.(22) with the particle fluctuating ener-

gy $\langle C_iC_i \rangle$, one can expect to overcome this defect. By comparing the two methods carefully, we adopted the latter in this study. Due to the lack of the support of experiment data, the modification here still needs to be validated, and the coupling relations need to be investigated in the future. Moreover, it is also difficult to deal with the boundary conditions of particle phase in solid/liquid system. There is no well-accepted method of it. The boundary treatment used in the present study proved successful in gas/solid flows[6,7]. But in solid/liquid flows the process of collisions between particles and the wall is slightly different from that in both gas/solid and granular flows due to the importance of the interphase forces. In addition, though the coefficients selected for the collisions are consistent with the previous investigations, they are not directly from the measured data in solid/liquid two-phase flows. Hence the treatment of boundary conditions, like the interphase coupling, remain worth studying.

4 Conclusions

Based on the preceding analysis and discussions, the main conclusions can be drawn as follows:

(1) Starting from the kinetic theory for solid/liquid two-phase flows and taking into account the external forces acting on a particle thoroughly, a mathematical model is established to predict the flow properties of particle phase in a square pipe. The predictions agree with the experiments very well.

(2) This model properly predicts two types of patterns of the vertical distribution of particle concentration observed in experiments. The cause of the formation of the two patterns is not only related to the lift force exerted on a particle, but also related to the characteristics of the vertical distribution of particle fluctuating energy.

(3) The predicted mean velocity of particles is smaller than the velocity of liquid in the core region, and may be larger than that of liquid near the pipe bottom. This result may relate to the only use of drag force and the boundary treatment.

(4) Similar to the vertical distribution of particle concentration, the particle fluctuating energy also shows different patterns. This is determined by the detailed two-phase flow conditions.

Acknowledgements This work was supported by the National Natural Science Foundation of China (Grant No. 59890200) and the Ministry of Water Resources.

References

1. Liu Dayou, Fluid Dynamics of Two-Phase Systems (in Chinese), Beijing: Higher Education Press, 1993.
2. Ni Jinren, Wang Guangqian, Zhang Hongwu, Basic Theories of Solid-Liquid Two-Phase Flows and Their Recent Applications (in Chinese), Beijing: Science Press, 1991.
3. Wang, G. Q., Ni, J. R., The kinetic theory for dilute solid/liquid two-phase flow, Int. J. Multiphase Flow, 1991, 17: 273.
4. Wang Guangqian, Ni Jinren, Kinetic theory for particle concentration distribution in two-phase flow, J. Eng. Mech., 1990, 116: 2738.
5. Ding, J. M., Gidaspow, D., A bubbling fluidization model using kinetic theory of granular flow, AIChE Journal, 1990, 36: 523.
6. Louge, M. Y., Mastorakos, E., Jenkins, J. T., The role of particle collisions in pneumatic transport, J. Fluid Mech., 1991, 231: 345.
7. Cao, J., Ahmadi, G., Gas-particle two-phase turbulent flow in a vertical duct, Int. J. Multiphase Flow, 1995, 21(6): 1203.
8. Jenkins, J. T., Savage, S. B., A theory for the rapid flow of identical, smooth, nearly elastic, spherical particles, J. Fluid

Mech., 1983, 130: 187.
9. Rizk, M. A., Elghobashi, S. E., On the motion of a spherical particle suspended in a turbulent flow near a plane wall, Phys. Fluids, 1985, 28: 806.
10. Crowe, C. T., Sommerfeld, M., Tsuji, Y., Multiphase Flows with Droplets and Particles, Florida: CRC Press, 1998
11. Owen, P. R., Pneumatic transport, J. Fluid Mech., 1969, 39: 407.
12. Wang Guangqian, The kinetic theory with experimental studies for the solid/liquid two-phase flow and granular flow, Ph. D. Thesis, Department of Hydraulic Engineering, Tsinghua Univ., Beijing, China, 1989.
13. Gidaspow, D., Multiphase Flow and Fluidization: Continuum and Kinetic Theory Descriptions, San Diego: Academic Press, 1994.
14. Koch, D. L., Kinetic theory for a monodisperse gas-solid suspension, Phys. Fluids A, 1990, 2: 1711.
15. Peirano, E., Leckner, B., Fundamentals of turbulent gas-solid flows applied to circulating fluidized bed combustion, Prog. Energy Combust. Sci., 1998, 24: 259.
16. Jenkins, J. T., Boundary conditions for rapid granular flow: flat frictional walls, J. Appl. Mech., 1992, 59: 120.
17. Dou, G. R., Turbulence (II) (in Chinese), Beijing: Higher Education Press, 1987.
18. Kulick, J. D., Fessler, J. R., Eaton, J. K., Particle response and turbulence modification in fully developed channel flow, J. Fluid Mech., 1994, 277: 109.
19. Alajbegovic, A., Assad, A., Lahey, R. T. Jr., Phase distribution and turbulence structure for solid/fluid upflow in a pipe, Int. J. Multiphase Flow, 1994, 20(3): 453.
20. Lee, S. L., Durst, F., On the motion of particles in turbulent duct flows, Int. J. Multiphase Flow, 1982, 8: 125.
21. Van de Wall, R. E., Soo, S. L., Measurement of transport properties of a gas-solid suspension using phase Doppler anemometry, Powder Technology, 1997, 94: 141.